# KINETIC MODELS FOR UPTAKE OF PESTICIDE (METHOMYL) FROM AQUEOUS SOLUTIONS USING  COTTON STALKS ACTIVATED CARBON

## M.S. El-Geundi, M.M Nassar, T.E. Farrag, M.S. Mahmoud[1], and M.H. Ahmed

*Department of Chemical Engineering, Faculty of Engineering, El-Minia University, 61516 El-Minia, Egypt.*
*1 Corresponding author, Tel.: +2-086-2364420, Fax: +2-086-2346674,*
*E-mail: m.salah.m@mu.edu.eg.*

## ABSTRACT

*Adsorption mechanism of methomyl onto activated carbon derived from cotton stacks (CSAC) was studied. A series of contact-time experiments have been undertaken in an agitated batch adsorber to assess the effect of design variables, namely, agitation speed, initial concentration, particle size range, and adsorbent mass. The batch kinetic experiments have been analyzed using both simplified surface diffusion model to determine external mass transfer coefficient, $k_s$, and the intraparticle diffusion model to determine macropore rate parameter, $k_i$. The kinetic studies strongly indicated that, the surface diffusion predominates in early stages of process (3% of process time) after that the intraparticle diffusion is the controlling step. Results showed that, the external mass transfer coefficient is directly proportional to agitation speed in contrast with other variables. The macropore rate parameter, $k_i$. was found to increase with the increase of agitation and initial concentration of mothomyl as an inverse with particle size and adsorbent mass. Agitation speed has more effect on external mass transfer than intraparticle coefficient. General correlations which relate both $k_s$ and $k_i$ with the design variables were obtained.*

## 1. INTRODUCTION

In Egypt like other many countries over the world, the agricultural activity occupies a very important place in the socio-economic domestic context which led to increase in using of  pesticides. Indiscriminate use of pesticides leads to the contamination of our environment (soils, surface and ground waters). Numerous cases of pesticide residue and ground water contamination have been reported in the literature[1,2]. Pesticides, which indeed seem indispensable for the nutrition of mankind, take a special place among the environmentally problematic substances. Small quantities of pesticides may enter the water environment through drift, leaching and run-off from nearby applications. The contamination of water of ponds, rivers and ground water sources with various insecticides and herbicides is posing a direct threat to human health. Therefore, the removal of pesticides from water is one of the major environmental concerns these days.

The insecticide (methomyl), $C_5H_{10}O_2N_2S$, is a broad spectrum insecticide which belongs to the carbamate family of pesticides. It is used for foliar treatment of vegetable specially tomato, fruit and field crops, cotton, commercial ornamentals, and in an around poultry houses and dairies.  It is produced by reacting *S*-methyl-*N*-hydroxylthio acetamidate (MHTA) in methylene chloride with gaseous methyl isocyanate at 30–35 °C. It has been classified by the WHO (World Health Organization), EPA (Environmental Protection Agency, USA) and EC (European Commission) as a very toxic and hazardous pesticide [3]. Methomyl pollutant causes environmental concerns because of its high solubility in water (57.9 g/L at 25 °C). Since sorption affinity of methomyl to soils is rather low, it can easily cause contamination of both ground and surface water resources. In addition, various

amounts of methomyl have been detected in surface and ground waters not only during actual insecticide application but also after a long period of use [4].

Several methods are available for pesticides removal such as photocatalytic degradation [5], advanced oxidation processes [6], aerobic degradation [7], nanofiltration membranes [8], ozonation [9] and adsorption [10, 11]. Advanced oxidation processes using hydrogen peroxides are, often ineffective because carbonate and bicarbonate ions, which are abundant in all natural water, react as strong free radical scavengers. The use of enzymes to detoxify wastewater failed to attract much attention due to the high cost of enzyme-based systems [12]. Filtration through membranes needs another method such as oxidation reaction catalyzed by enzyme to transform the pesticide into an insoluble product, so that this method is highly expensive. Compared with the above methods, adsorption on activated carbon is the most widespread technology used to deal with purification of water contaminated by pesticides [13], dyes [14] and phenols [15], etc. It allows flexibility in design and operation and produces aesthetically superior effluents suitable for reuse.

Commercially available activated carbons are still considered expensive due to the use of non-renewable and relatively expensive starting material such as coal. This has led a growing research interest in the production of activated carbons from renewable and cheaper precursors. The ability of cotton stalks activated carbon as an adsorbent to remove methomyl from aqueous solution was evaluated from the equilibrium studies in a batch adsorption system [16]. The annual production of cotton stack in Egypt as a waste product was 1.2 million tons in 2012 where any attempt to reutilize this waste will be useful. Therefore, the purpose of this work is to study the mechanism of methomyl adsorption onto the locally prepared cotton stalks activated carbon (CSAC) in order to assess the effect of design variables, namely agitation speed (rpm), methomyl initial concentration ($C_0$), adsorbent dose (m) and particle size ($d_p$). In general the adsorption process involves multi-steps mainly the surface diffusion followed by the intraparticle diffusion. From mechanistic view point it is necessary to identify the steps involved during adsorption, described by external mass transfer (boundary layer diffusion) and intraparticle diffusion. As the double nature of the adsorption process, both the external mass transfer coefficient $k_s$, and the intraparticle diffusion coefficient $k_i$ was determined and correlated as a function of the design variables.

## 2. ADSORPTION MECHANISM

It is necessary to study the kinetics of adsorption in batch systems in order to determine the rate-limiting step in the process. It was proposed that the mechanism of methomyl adsorption onto CSAC consists of several steps. However, for the purposes of this work the overall adsorption process is assumed to occur by the following three steps:
   a. Mass-transfer of the methomyl from the bulk solution to the particle surface (external mass-transfer);
   b. Intraparticle diffusion of methomyl via either a pore diffusion, or a homogeneous solid-phase diffusion;
   c. Adsorption at an interior site.

During the establishment of the rate-limiting step, step (iii) is assumed to be rapid and hence not considered in kinetic analysis in this work. Consequently, the two possible rate-limiting steps considered are external mass-transfer and intraparticle diffusion. The development of models based on two such mass transport steps occurring simultaneously is quite complex, requiring a coupling equation and its subsequent solution. Therefore, simplifying assumptions have been made and attempts undertaken to describe the adsorption processes in terms of either an external-mass transfer coefficient or an internal (intraparticle diffusion) mass-transfer parameter [17].

## 3. MATERIAL AND PROCEDURES

### 3.1 Materials

The adsorbate used in this study was the an insecticide, methomyl, (S-methyl N-[(methylcarbamoyl)oxy] thioacetimidate). The physicochemical properties of methomyl are shown in Table 1. The methomyl was supplied by Egyptian Company for commerce and agriculture, Egypt. The concentrations of methomyl solutions were measured by a UV- Spectrophotometer (Shimadzu, Inc. kyoto Japan model U.V-1601). All measurements were made at the wavelength corresponding to maximum absorbance, $\lambda_{max}$, which is 233 nm. Synthetic stock solutions were prepared by dissolving accurately weighed amounts methomyl in 1 L of distilled water. The desirable experimental concentrations of solutions were prepared by diluting the stock solution with distilled water when necessary.

The adsorbent used in this study is a locally activated carbon prepared in our laboratories from cotton stalks which collected from El- Minia governorate, Egypt. The sun-dried cotton stalks was crushed and sieved onto three ranges of particle sizes, (0.6:1mm), (1:2mm) and (2:4mm). The raw material (40 g) were impregnated with concentrated solution of ortho- phosphoric acid (0.2 dm$^3$) of pre-adjusted concentrations, this amount of acid solution was found to be sufficient to cover the whole mass and to give a paste of soft consistency (weight ratio of 2PA:1CS). The carbonization and activation were completed by heating the mixture for 12h in an air oven until complete evaporation of the excess water and to facilitate the absorption of phosphoric acid by the raw material. The resulting material was transferred to the stainless steel reactor placed inside the tubular furnace attached with a thermocouple for temperature control. To avoid splashing caused by vigorous evolution of gases, temperature was increased slowly at rate of 7ºC/min. at constant flow of nitrogen. After sample temperature reached to 500ºC, it was left for 2 h at this temperature then allowed to cool to a room temperature in nitrogen atmosphere. The resulting carbon was washed with distilled water till a constant pH of the slurry was reached, then deride at 100 ºC overnight in an air oven, ground and sieved. More details about CSAC are presented in a previous work [16].

**Table 1. Physicochemical properties of methanol [17].**

| Property | Parameter value |
|---|---|
| Chemical structure | $CH_3-C=N-O-\overset{\overset{\displaystyle O}{\|}}{C}-N\overset{\diagup H}{\diagdown CH_3}$ , $\overset{\|}{S}-CH_3$ |
| CAS number | 16752 - 77 - 5 |
| Chemical formula | $C_5H_{10}N_2O_2S$ |
| Molecular weight | 162.21 g/mol |
| Molecular volume | 179.9 cm$^3$/mol |
| Colure | White crystalline solid |
| Sp.gr at 298.15 K, ( - ) | 1.29 |
| Solubility in water at 298.15 K | 58,000 mg/L |
| Log octanol/water partition coefficient, log $K_{ow}$ | 0.60 |
| Log soil organic carbon-water partitioning coefficient | 2.6 |
| Melting point, K | 351.15 - 316.15 |
| Vapor pressure at 298.15 K, mm Hg | 5.4($10^{-6}$) |

### 3.2 Procedures

In order to investigate the influence of system variables on the adsorption rate, a batch adsorber vessel with a standard tank configuration was used in all experiments. The batch adsorber was a baffled 1.5 dm$^3$ prespex vessel and holding a volume of 1.25 dm$^3$ methomyl solution in each run. Constant and uniform agitation was achieved using a variable speed motor and a six bladed (flat) prespex impeller. Eight prespex baffles were evenly spaced around the circumference of the adsorber. Initially measurements were taken as short intervals for the first 2-5 min, to calculate the external mass-transfer coefficient. Thereafter measurements were made at increasing intervals until equilibrium was reached. The amount of adsorption $q_t$ (mg/g), at time t (min.), was calculated by:

$$q_t = V(C_0 - C_t)/m \tag{1}$$

where $C_t$ (mg/l) is concentrations of methomyl at time t.

The model presented for determining the external mass-transfer coefficient, $k_s$, is based on work by Furusawa and Smith [18]. It assumes that the external mass transport of the methomyl from the bulk solution across the boundary layer film to the external particle surface is rate-controlling in the early stages of the adsorption process. In a well-agitated batch adsorber mixing in the liquid phase is rapid, hence the concentration of adsorbate in the liquid phase ($C_t$) and the concentration of adsorbent particles in the liquid ($m_s$) are assumed uniform throughout the vessel. Since at time t=0, all the mass transfer resistance is restricted to the external layer of the particle.

The change in methomyl concentration ($C_t$) with time is related to the fluid-particle mass-transfer coefficient by the equation:

$$\left\lfloor \frac{d(C_t)}{dt} \right\rfloor_{t=0} = -k_s S_s (C_t - C_s), \quad \text{where, } C_t = C_0 \quad \text{at} \quad t = 0 \tag{2}$$

If the effective diffusion coefficients are neglected, since $C_s$ approaches zero and $C_t$ approaches $C_0$ as $t \to 0$, then:

$$\left\lfloor \frac{d(C_t/C_0)}{dt} \right\rfloor_{t=0} = -k_s S_s \tag{3}$$

Hence, the slope at t = 0 of a plot of ($C_t/C_0$) versus time is equal to (- $k_s S_s$), and $k_s$ can be extracted from such a slope, where external surface area of particles, $S_s$, can be obtained by assuming that the particles are spherical of diameter, $d_p$, hence:

$$S_s = \frac{6(m/V)}{dp\rho_t.(1-\varepsilon_p)} \tag{4}$$

The second model is the intraparticle diffusion model proposed by Weber and Morris [19] which can be written as follow:

$$q_t = k_i t^{0.5} + Z \tag{5}$$

where $q_t$ (mg/g) is the amount adsorbed at time, $t^{0.5}$ is the square root of the time (min$^{0.5}$), $k_i$ (mg/g.min$^{0.5}$) is the rate constant of intraparticle diffusion. Z is the value of the intercept, which gives an idea about the boundary layer thickness, i.e., the larger the intercept; the

greater is the boundary layer effect. The plots of $q_t$ vs $t^{0.5}$ would give straight lines whose slopes provide the intraparticle diffusion coefficients to be obtained ($k_i$).

Values of $k_s$ and $k_i$ calculated at different design variables were correlated in a general form as:

$$k_s \, or \, k_i = A(rpm)^B (C_0)^D (d_p)^E (m)^F \qquad (6)$$

where A , B, D, E and F are constants.

## 4. RESULTS AND DISCUSSION

### 4.1. External Mass Transfer Model

Figure (1L) shows the experimental results obtained from a series of contact time studies in which the degree of agitation was varied from 50 to 500 rpm as a plot of ($C_t/C_0$) against time where other parameters remain fixed. The initial gradients $(d(C_t/C_0)/dt)_{t\,=\,0}$ of the various curves have been determined which is equal to ($-k_s S_s$), from such slopes, $k_s$ can be extracted as described in Eq. (3).
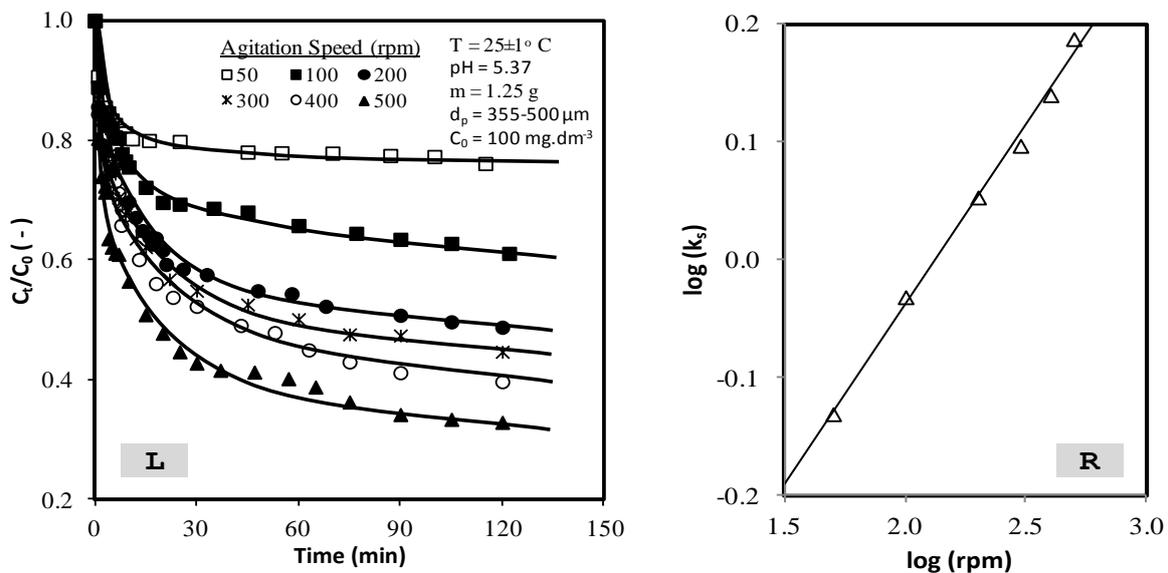


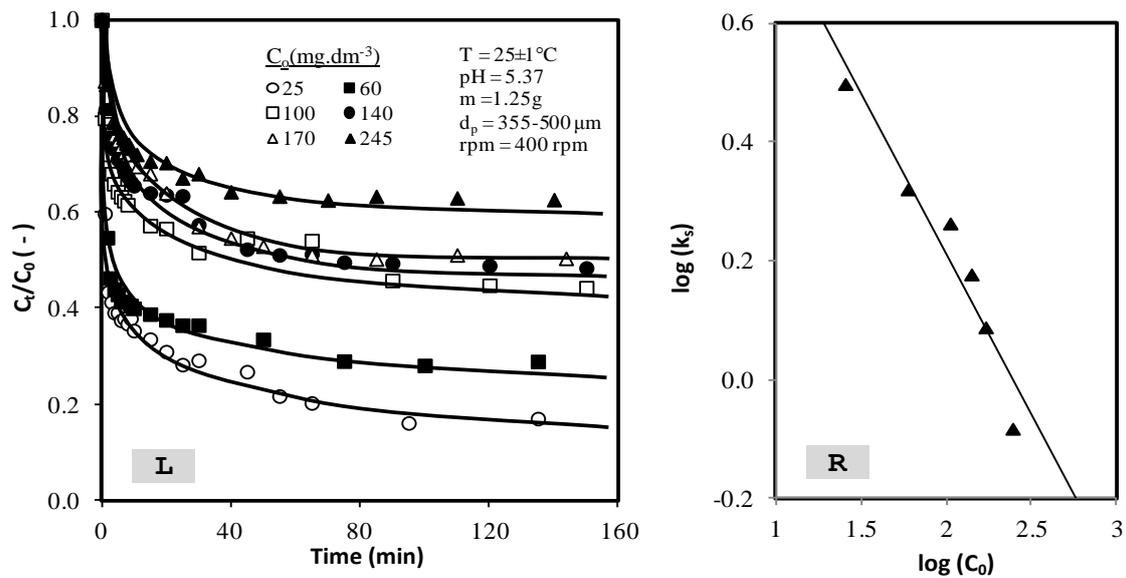**Fig.1: (L) Typical time-concentration ratio at different agitation speeds, (R) plot of log $k_s$ versus log rpm for adsorption of methomyl onto CSAC.**

The results indicate that, removal of methomyl increases with agitation speed. The increase in the extent of removal can be explained on the following basis: (a) the solute species (methomyl) may get activated due to a gain in kinetic energy and easily cross the potential barrier, (b) increase in agitation speed decreases the boundary layer resistance to mass transfer in the bulk solution.

The external mass-transfer coefficients, $k_s$, calculated for different agitation speeds (presented in Table 2) have been plotted as log $k_s$ against log rpm, Fig. (1R). A linear variation was observed which indicate that, the external adsorption of methomyl onto CSAC is controlled by the degree of agitation and that the effect of increasing agitation is to decrease the boundary layer resistance to mass transfer and hence increase the mobility of the solid/fluid system.

The major controlling factor in external mass transfer is the thickness of the boundary layer, Since all experiments were undertaken at 400 rpm to achieve completely mixed systems. Consequently,

there was a considerable shear force on the boundary layer which made this initial resistance to mass transfer fairly low, and hence the intrinsic adsorption rate was very rapid until an external surface coverage of methomyl had occurred on the carbon particles.

The influence of initial methomyl concentration has also been studied and the experimental results are depicted in Fig. (2L). The external mass-transfer coefficients, $k_s$, have been determined as mentioned before and these results have also been plotted as log $k_s$ versus log $C_0$ where a linear variation was observed, Fig. (2R). The driving force for mass transfer (based on the difference between the bulk liquid concentration and the particle surface liquid concentration) is time dependent. This concentration difference, relative to $C_0$, will affect the way in which the external mass-transfer coefficient varies with methomyl concentration. Thus, the external mass transfer coefficients decrease as $C_0$ increases for methomyl being adsorbed onto natural clay (Table 2).



**Fig.2: (L) Typical time-concentration ratio at different initial concentrations, (R) plot of log $k_s$ versus log $C_0$ for adsorption of methomyl onto CSAC.**

The third variable which effect on the rate of mass transfer is the adsorbent particle size, $d_p$. The influence of contact time on different ranges of particle size of CSAC has also been investigated using different six particle size ranges from 125 to 1000 μm. The experimental data are presented in Fig. (3L) where the effect are presented in Fig. (3R). The results show an increase in the rate of methomyl uptake as the mean diameter ($d_p$) decreases. This observation is in agreement with the proposed mechanism, since a large external surface area (for small particles) removes more methomyl during the initial stages of the adsorption process than large particles.
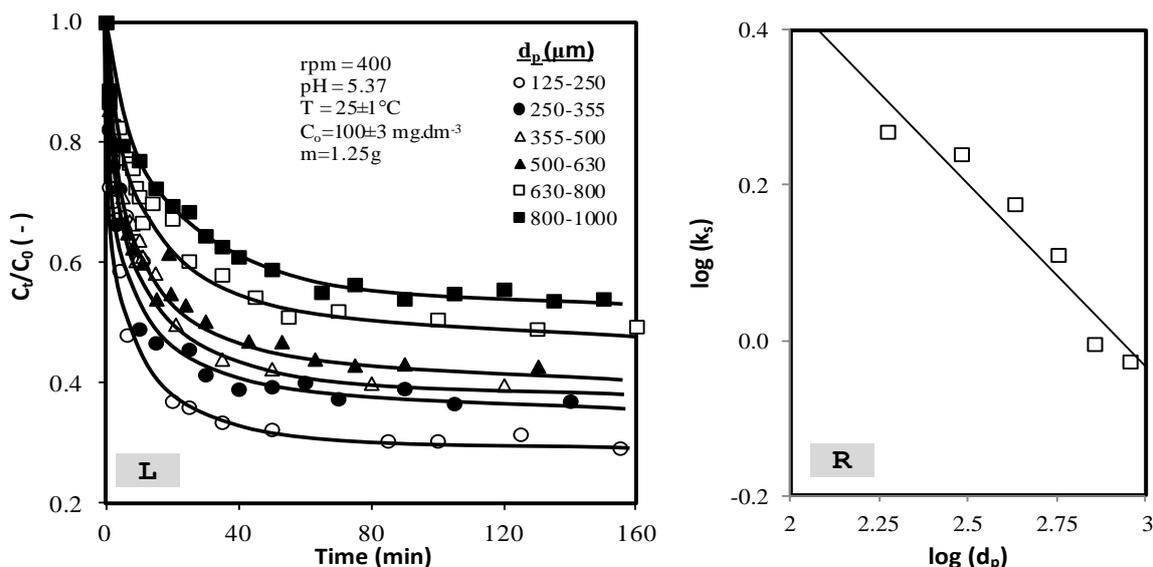
**Fig. 3: (L) Typical time-concentration ratio at different particle size ranges, (R) plot of log $k_s$ versus log $d_p$ for adsorption of methomyl onto CSAC.**

The external mass-transfer coefficients, $k_s$, for different particle size ranges have been obtained and listed in Table 2. The data demonstrate that a decrease in the mean particle diameter ($d_p$), results in an increase in the external mass-transfer coefficient, $k_s$. This can be explained by the fact that the smaller particles move faster in solution than larger particles and thus there is more shear on their surfaces. As a result, the boundary layer thickness is thinner than that on the larger particles, and as a consequence $k_s$ increases as $d_p$ decreases. Since there are more small particles per unit mass in solution (relative to large diameter particles) there will be a greater shearing effect due to collisions and intraparticle interactions, which again supports the observation that $k_s$ increases as $d_p$ decreases.

**Table 2. Values of external mass transfer coefficient, $k_s$, at different operating variables for the adsorpion of methomyl onto CSAC.**

| Parameters | Values | | | | | |
|---|---|---|---|---|---|---|
| Speed (rpm) | 50 | 100 | 200 | 300 | 400 | 500 |
| $k_s$ | 0.74 | 0.93 | 1.13 | 1.25 | 1.41 | 1.54 |
| $C_0$ (mg/l) | 25.4 | 59.3 | 105.2 | 140.2 | 170.4 | 245.4 |
| $k_s$ | 3.16 | 2.10 | 1.48 | 1.51 | 1.23 | 0.83 |
| $d_p$ (μm) | 187.5 | 302.5 | 427.5 | 565.0 | 715.0 | 900.0 |
| $k_s$ | 1.86 | 1.74 | 1.45 | 1.29 | 0.99 | 0.94 |
| m (g) | 0.50 | 0.75 | 1.0 | 1.25 | 0.50 | 2.0 |
| $k_s$ | 2.16 | 1.70 | 1.61 | 1.43 | 1.32 | 1.20 |

The influence of adsorbent mass (dose) on mass transfer has been studies also in this research where other experimental conditions keeping constant, Fig. (4L). The initial gradients of the various curves allow to determine $k_s$ for different adsorbent masses and listed in Table 2. The results have been plotted as log $k_s$ versus log m and a linear behaviour is obtained, Fig. (4R). The resulting behaviour indicates that $k_s$ varies with the mass of adsorbent in a logarithmic manner.

The external mass-transfer coefficient depends on the driving force per unit area, and in this case, since $C_0$ and $d_p$ are constant, increasing mass of CSAC will increases the surface area for adsorption, hence, the rate of methomyl uptake increases. The $k_s$ values listed in Table 2 for different dosages indicate only a small dependence on mass with an inverse proportional. This effect is probably due

to the fact that for small masses a small amount of external surface is presented to the methomyl and therefore there is a large driving force from the methomyl per unit surface area of CSAC.
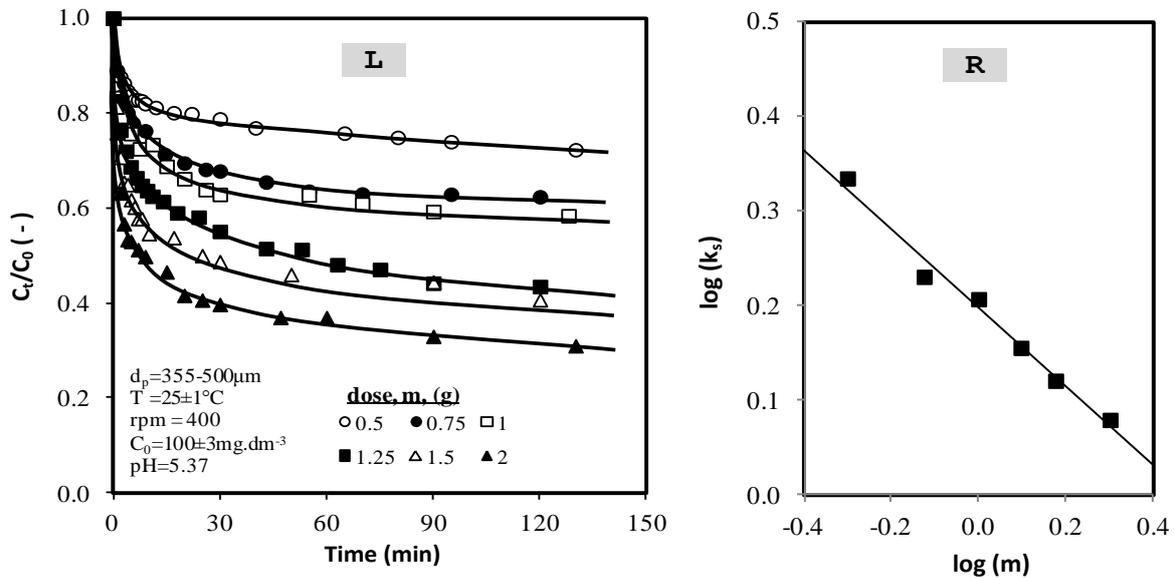


**Fig. 4: (L) Typical time-concentration ratio at different adsorbent masses, (R) plot of log $k_s$ versus log m for adsorption of methomyl onto CSAC.**

The experimental data of external mass transfer coefficient, $k_s$, which obtained for different studied variables (agitation speed, initial concentration, particle size and the mass of CSAC) was correlated in a general form as follow,

$$k_s = 6.42(rpm)^{0.45}(C_0)^{-0.35}(d_p)^{-0.41}(m)^{-0.43} \tag{7}$$

## 4.2. Intraparticle Diffusion Model

Intraparticle diffusion model is the second model used to describe the mechanism of methomyl uptake from its aqueous solution using CSAC. The intraparticle diffusion coefficient $k_i$, will be determined from the plot of methomyl solid phase concentration ($q_t$), against the square root of time ($t^{0.5}$). Overall, in the present work, the plot of $q_t$ versus $t^{0.5}$ has a characteristic shape, composed of three separate portions. The initial portion (shady area) is due to external-mass transport effects, followed by the effect of intraparticle diffusion (linear portion), which generally predominates from 3% to at least 97% of the adsorption time. This is followed by a decreased rate of diffusion, which is observed as a second linear portion, leading eventually to an equilibrium plateau. This is explained by the decrease of bulk solute concentration and surface solute concentration.

Figure (5L) represent plotting of methomyl solid phase concentration ($q_t$), against the square root of time ($t^{0.5}$) at different agitation speed ranged from 50 to 500 rpm when other operating parameters are fixed. Plots for the effect of other parameters ($C_0$, $d_p$, and m) are not present and approximately has the same configuration. The intraparticle diffusion coefficient $k_i$ have been determined from the slope of the first linear portions at various levels of agitation speed and are listed in Table 3. In all cases, the $k_i$ values are increasing slightly with an increase in the agitation speed, where the resulting behaviour indicates that $k_i$ varies with rpm in a logarithmic manner, Fig. (5R). The explanation probably arises from the fact that the adsorption process is a two-step mechanism involving external-mass transfer as well as intraparticle diffusion. Enhanced agitation rates will decrease the film resistance, enabling the methomyl to concentrate more rapidly at the particle surface and consequently there will be a greater driving force for intraparticle diffusion and thus higher $k_i$ values.
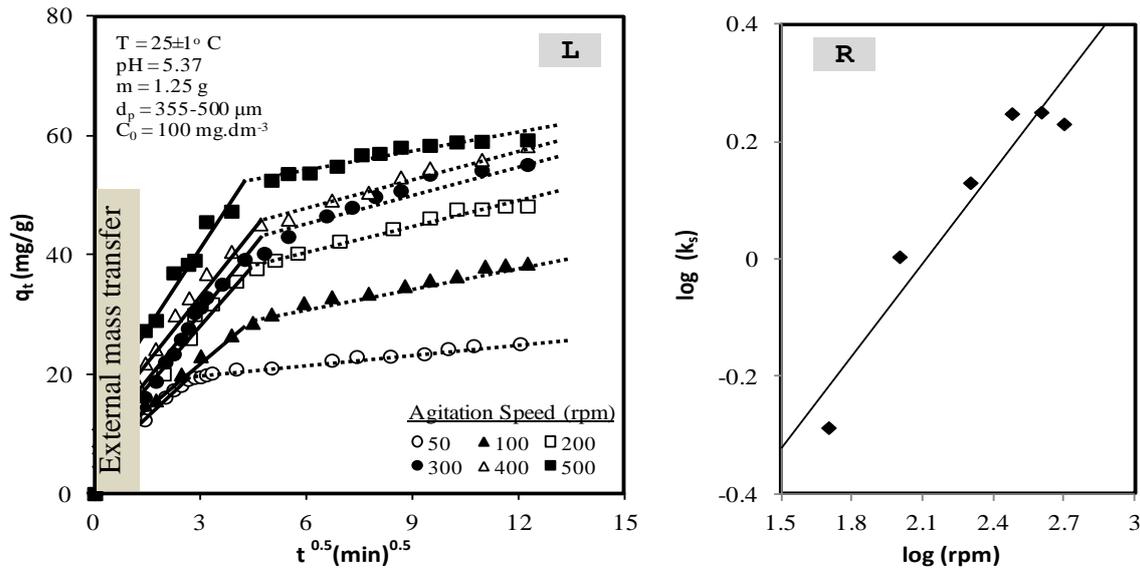
**Fig. 5: (L) Plot of $q_t$ against $t^{0.5}$ for various agitation speeds, (R) plot of log $k_i$ against log rpm during the adsorption of methomyl onto CSAC.**

The results in Table 3 show that there is a gradual increase in $k_i$ with an increase in $C_0$ indicating that increasing the bulk liquid concentration increases the driving force of methomyl from the bulk solution and then into the solid particle. The influence of particle size on $k_i$ has an inverse proportion. It has been postulated that if the mechanism of methomyl removal is one of adsorption onto the external sites of a porous adsorbent, the rate of uptake and hence the macropore rate parameter, $k_i$, should vary reciprocally with power of the diameter for a given mass of adsorbent. In general, the $k_i$ value decreases slightly with increasing mass of CSAC. For a given particle size, increasing the mass increases the surface area for mass transfer. Thus the mass transfer per unit surface area will be decreased, due to the increased surface area available. Results of intraparticle diffusion coefficient $k_i$ was correlated with the design variables according to Eq. 6 as follow,

$$k_i = 0.29 (rpm)^{0.31} (C_0)^{0.53} (d_p)^{-0.44} (m)^{-0.25}$$
(8)

**Table 3. Values of intraparticle mass transfer coefficient, $k_i$, at different operating variables for the adsorpion of methomyl onto CSAC.**

| Parameters | Values | | | | | |
|---|---|---|---|---|---|---|
| Speed (rpm) | 50 | 100 | 200 | 300 | 400 | 500 |
| $k_i$ | 0.517 | 1.01 | 1.35 | 1.77 | 1.78 | 1.70 |
| $C_0$ (mg/l) | 25.4 | 59.3 | 105.2 | 140.2 | 170.4 | 245.4 |
| $k_i$ | 0.36 | 0.57 | 1.32 | 1.78 | 1.93 | 2.78 |
| $d_p$ (µm) | 187.5 | 302.5 | 427.5 | 565.0 | 715.0 | 900.0 |
| $k_i$ | 2.28 | 1.80 | 1.66 | 1.31 | 1.09 | 1.09 |
| m (g) | 0.50 | 0.75 | 1.0 | 1.25 | 0.50 | 2.0 |
| $k_i$ | 0.22 | 0.17 | 0.16 | 0.14 | 0.13 | 0.12 |

The validation of predicted correlations, Eqs. 7 & 8, using 45° line where the experimental data are plotted against values predicted from correlations is shown in Fig. 6. All values approximately fall on the line, i.e both measured and predicted values in agreement means the correlations simulate the experimental data well.
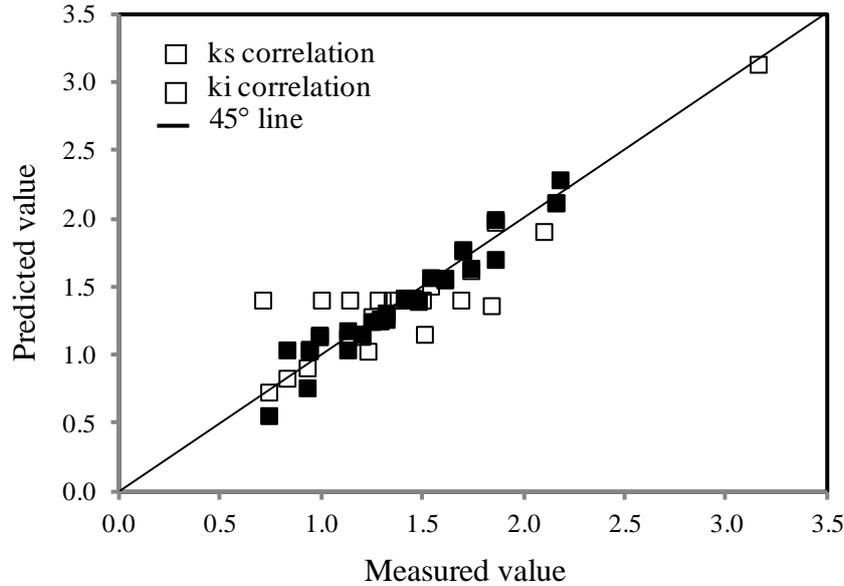
**Fig. 7: Comparison between measured and predicted values for both correlations of surface and intraparticle diffusion models**

## 5. CONCLUSIONS

The kinetics of methomyl adsorption onto CSAC has been studied at different design parameters namely: agitation speed, initial methomyl concentrations, adsorbent size, and adsorbent mass. The kinetic studies indicated that the external mass-transfer is the rate-controlling step in early stages of the adsorption process and the deviation thereafter is due to the development of intraparticle diffusion resistance. Both external mass-transfer coefficient ($k_s$) and the macropore rate parameter ($k_i$) has been measured when design variables ware varied. The experimental data for both $k_s$ and $k_i$ are correlated with design variables in a general form as:

$$k_s = 6.42(rpm)^{0.45}(C_0)^{-0.35}(d_p)^{-0.41}(m)^{-0.43} ,$$

$$k_i = 0.29(rpm)^{0.31}(C_0)^{0.53}(d_p)^{-0.44}(m)^{-0.25}$$

Inspection of the above two equations, proves that agitation has more influence on external mass transfer coefficient, $k_s$, since power of rpm in case of external coefficient is greater than that of intraparticle coefficient.

## REFERENCES

[1]. Chang C., Lee S., Adsorption behavior of pesticide methomyl on activated carbon in a high gravity rotating packed bed reactor, *Water research,* Vol. 46, pp. 2869-2880, 2012.

[2]. Tomasevic A., Kiss E., Petrovic S., Study on the photocatalytic degradation of insecticide methomyl in water, *Desalination,* Vol. 262, pp. 228-234, 2010.

[3]. Bouzaida I., Ferronato C., Chovelon J.M., Rammah M. E. and Herrmann J.M., Heterogeneous photocatalytic degradation of the anthraquinonic dye, Acid Blue 25 (AB25): a kinetic approach, *J. Photochem. Photobiol.,* Vol. 168 (1-2), pp. 23-30, 2004.

[4]. Tomlin C.D.S., *The Pesticide Manual*, 13 Ed, BCPC, Hampshire, pp. 697-698, 2006.

[5].  Aungpradit T., Sutthivaiyakit P., Martens D., Sutthivaiyakit S., Kettrup F., Photocatalytic degradation of triazophos in aqueous titanium dioxide suspension: identification of intermediates and degradation pathways. *J. Hazard. Mater.*, Vol.  146,  pp. 204-213, 2007.

[6].  Saritha P., Aparna C., Himabindu V., Anjaneyulu Y., Comparison of various advanced oxidation processes for the degradation of 4-chloro-2 nitrophenol, *J. Hazard. Mater.,* Vol.  149, pp. 609-614, 2007.

[7].  Rajashekara Murthy H.M., Manonmani H.K., Aerobic degradation of technical hexachlorocyclohexane by a defined microbial consortium., *J. Hazard. Mater.,* Vol.  149, pp. 18-25, 2007.

[8].  Ahmad A.L., Tan L.S., Shukor S.R.A., Dimethoate and atrazine retention from aqueous solution by nanofiltration membranes, *J. Hazard. Mater.*, Vol.  151, pp. 71-77, 2008.

[9].  Maldonado M.I., Malato S., Pérez-Estrada L.A., Gernjak W., Oller I., Doménech X., Peral J., Partial degradation of five pesticides and an industrial pollutant by ozonation in a pilot-plant scale reactor, *J. Hazard. Mater.*, Vol. 38, pp. 363-369, 2006.

[10].Chang C.F., Chang C.Y., Hsu K.E., Lee S.C., Adsorptive removal of the pesticide methomyl using hypercrosslinked polymers, *J. Hazard. Mater.*, Vol.  155, pp. 295-304, 2008.

[11].Gupta V.K., Suhas I., Saini V.K., Adsorption of 2,4-d and carbofuran pesticides using fertilizer and steel industry wastes. *J. Colloid Interface Sci.*, Vol.  299, pp. 556-563, 2006.

[12].Bonne P., Beerendonk E.F., Hoek V.J., Hofman J., Retention of herbicides and pesticides in relation to aging of RO membranes. *Desalination,* Vol. 132, pp. 189-194, 2000.

[13].Hamadi N.K., Swaminathan S., Chen X.D., Adsorption of Paraquat dichloride from aqueous solution by activated carbon derived from used tires. *J. Hazard. Mater.*, Vol. 112, pp. 133-141, 2004.

[14].Hameed B.H., Ahmad A.L., Latiff K.A., Adsorption of basic dye (methylene blue) onto activated carbon prepared from rattan sawdust. *Dyes Pigments*, Vol. 75, pp. 143-149, 2007.

[15].Tan I.A.W., Ahmad A.L., Hameed B.H., Adsorption of basic dye using activated carbon prepared from oil palm shell: batch and fixed bed studies. *Desalination*, Vol. 225, pp. 13-28, 2008.

[16].El-Geundi M.S., Nassar M.M, Farrag T.E., Ahmed M.H., Methomyl Adsorption onto Cotton Stalks Activated Carbon (CSAC): Equilibrium and Process Design, *Procedia Environmental Science*, Vol. *17,  pp.* 630-639, 2013.

[17].Hazardous Substances Data Bank (HSDB), http://toxnet.nlm.nih.gov/, retrieved 30/6/2013

[18].Furusawa T., Smith J.M., Fluid-particle and intraparticle mass transport rates in slurries,  *Ind. Eng. Chem. Fundam.*, Vol. 12, Part2, pp.197-203, 1973a.

[19].Weber W.J., Morris J.C., Kinetics of adsorption on carbon from solution, *J. Sanitary Eng. Div. Proceed. Am. Soc. Civil Eng.,* Vol. 89, pp. 31-59, 1963.